

# Criteria and Methods for Estimating External Effective Dose Equivalent from Personnel Monitoring Results

*EDE Implementation Guide*

---

# **Criteria and Methods for Estimating External Effective Dose Equivalent from Personnel Monitoring Results**

EDE Implementation Guide

**TR-109446**

Final Report, September 1998

EPRI Project Manager

C. Hornibrook

## **DISCLAIMER OF WARRANTIES AND LIMITATION OF LIABILITIES**

THIS REPORT WAS PREPARED BY THE ORGANIZATION(S) NAMED BELOW AS AN ACCOUNT OF WORK SPONSORED OR COSPONSORED BY THE ELECTRIC POWER RESEARCH INSTITUTE, INC. (EPRI). NEITHER EPRI, ANY MEMBER OF EPRI, ANY COSPONSOR, THE ORGANIZATION(S) NAMED BELOW, NOR ANY PERSON ACTING ON BEHALF OF ANY OF THEM:

(A) MAKES ANY WARRANTY OR REPRESENTATION WHATSOEVER, EXPRESS OR IMPLIED, (I) WITH RESPECT TO THE USE OF ANY INFORMATION, APPARATUS, METHOD, PROCESS, OR SIMILAR ITEM DISCLOSED IN THIS REPORT, INCLUDING MERCHANTABILITY AND FITNESS FOR A PARTICULAR PURPOSE, OR (II) THAT SUCH USE DOES NOT INFRINGE ON OR INTERFERE WITH PRIVATELY OWNED RIGHTS, INCLUDING ANY PARTY'S INTELLECTUAL PROPERTY, OR (III) THAT THIS REPORT IS SUITABLE TO ANY PARTICULAR USER'S CIRCUMSTANCE; OR

(B) ASSUMES RESPONSIBILITY FOR ANY DAMAGES OR OTHER LIABILITY WHATSOEVER (INCLUDING ANY CONSEQUENTIAL DAMAGES, EVEN IF EPRI OR ANY EPRI REPRESENTATIVE HAS BEEN ADVISED OF THE POSSIBILITY OF SUCH DAMAGES) RESULTING FROM YOUR SELECTION OR USE OF THIS REPORT OR ANY INFORMATION, APPARATUS, METHOD, PROCESS, OR SIMILAR ITEM DISCLOSED IN THIS REPORT.

ORGANIZATION(S) THAT PREPARED THIS REPORT

**ENCORE Technical Resources, Inc.**

## **ORDERING INFORMATION**

Requests for copies of this report should be directed to the EPRI Distribution Center, 207 Coggins Drive, P.O. Box 23205, Pleasant Hill, CA 94523, (510) 934-4212.

Electric Power Research Institute and EPRI are registered service marks of the Electric Power Research Institute, Inc. EPRI. POWERING PROGRESS is a service mark of the Electric Power Research Institute, Inc.

Copyright © 1998 Electric Power Research Institute, Inc. All rights reserved.

## CITATIONS

---

This report was prepared by

ENCORE Technical Resources, Inc.

29 N. Union Street

Middletown, PA 17057

Principal Investigators

D. Owen

This report describes research sponsored by EPRI.

The report is a corporate document that should be cited in the literature in the following manner:

*Criteria and Methods for Estimating External Effective Dose Equivalent from Personnel Monitoring Results: EDE Implementation Guide*, EPRI, Palo Alto, CA: 1998. Report TR-109446.



# REPORT SUMMARY

---

Revisions to the radiation protection standards contained in Title 10, Part 20 of the Code of Federal Regulations require nuclear power plants to assess a worker's "effective dose equivalent" (EDE). This report is a concise summary of EPRI's EDE research and presents some simple guidelines on how the EDE methodology can be implemented at nuclear power plants.

## Background

In 1977, to account for human organ and tissue differences, the International Commission on Radiological Protection (ICRP) proposed specific organ radiation exposure weighting factors—in essence, risk-based radiation dose limits. These and other aspects of the ICRP recommendations were adopted in revisions made in 1991 to 10 CFR 20. The regulations require licensees to evaluate EDE using the very conservative assumption that the weighting factor for external exposure is one. However, the regulations allow licensees to propose alternative methods for evaluating the external radiation component of effective dose equivalent.

## Objectives

- To describe EPRI's effective dose equivalent research
- To explain EPRI's methodology for assessing effective dose equivalent
- To present some simple guidelines illustrating how the methodology could be used at nuclear power plants

## Approach

Researchers performed Monte Carlo calculations of photon transport through the human body. They used mathematical models of the human adult male and female and, for a variety of external radiation sources, calculated energy deposition in a large number of human organs and tissues. Using published organ weighting factors, they calculated effective dose equivalents for these irradiations. They determined how EDE varies with photon energy for various beam source geometries and for point sources both on and off the body. Calculations were made of photon energy fluence on the surface of the body as a function of location, source geometry, and photon energy. These results allowed researchers to understand how dosimeter placement affects EDE assessments.

---

## **Results**

Research showed that for beam sources, beams striking the front of the body normal to the body's major axis (i.e., straight on) produce the largest effective dose equivalent. The next highest effective dose equivalent are produced by beams striking the rear of the torso, again normal to the body's major axis. Effective dose equivalent falls significantly if the incident radiation departs from these two orientations. For point sources in contact with the body, the effective dose equivalent is highest for females when the source is on the front of the torso near the sternum. For males, it is highest when the source is on the front of the torso near the gonads. The widespread practice of supplementing a single front-worn dosimeter with additional dosimeters placed facing a radiation source should be abandoned, as this can significantly overestimate EDE. Using a single front-worn dosimeter as a measure of EDE is acceptable. Simple algorithms applied to two dosimeters (on the front and back) yield an accurate and numerically lower EDE under most all radiation exposure situations.

## **EPRI Perspective**

EPRI's EDE research showed that external effective dose equivalent should be evaluated using the organ weighting factors allowed for internal exposures and that doing so would not underestimate external EDE. EPRI believes its EDE methodology is an acceptable alternative method for assessing EDE from occupational radiation exposure.

Considerable benefits can be derived by U.S. nuclear utilities if they develop a technically rigorous approach for determining effective dose equivalents for their workforces. Their approach should be generally conservative, be acceptable to regulatory agencies, and be consistent with existing dosimetry practices. This methodology appears to meet these criteria.

## **TR-109446**

### **Interest Categories**

Nuclear plant operations  
Radiation protection technology  
Occupational radiation control

### **Keywords**

Effective dose equivalent  
Radiation exposure  
Photon radiation  
Dosimetry  
10 CFR 20

# ABSTRACT

---

Title 10 Part 20 of the Code of Federal regulations requires that nuclear power plant licensees evaluate worker radiation exposure using a risk-based methodology termed the "effective dose equivalent" (EDE). EDE is a measure of radiation exposure that represents an individual's risk of stochastic injury from their exposure.

EPRI's has conducted research into how photons interact with the body. These results have been coupled with information on how the body's organs differ in their susceptibility to radiation injury, to produce a methodology for assessing the effective dose equivalent. The research and the resultant methodology have been described in numerous technical reports, scientific journal articles, and technical meetings.

EPRI is working with the Nuclear Energy Institute to have the EPRI effective dose equivalent methodology accepted by the Nuclear Regulatory Commission for use at U.S. nuclear power plants. In order to further familiarize power plant personnel with the methodology, this report summarizes the EDE research and presents some simple guidelines for its implementing the methodology.



## ACKNOWLEDGMENTS

---

W.D. Reece (Texas A&M University) conducted the effective dose equivalent research described herein. Ralph Andersen (Nuclear Energy Institute) suggested that this short summary of the EDE methodology and the concise implementation guidelines be written, and made many comments and suggestions. Finally, EPRI would like to thank the many health physicists and radiation protection specialists from nuclear utilities who reviewed this document and made numerous suggestions for improvement.



# CONTENTS

---

<b>1 INTRODUCTION .....</b>	<b>1-1</b>
<b>2 BACKGROUND.....</b>	<b>2-1</b>
2.1 Origin and Basis of Effective Dose Equivalent.....	2-1
2.2 Current Regulatory Framework.....	2-2
2.3 Research Summary .....	2-3
Beam Sources.....	2-5
Point Sources in Contact With the Torso .....	2-5
Point Sources Away From the Torso.....	2-5
Surface Flux Measurements (Dosimeter Simulations).....	2-6
<b>3 EFFECTIVE DOSE EQUIVALENT METHODOLOGY .....</b>	<b>3-1</b>
3.1 Single Dosimeter EDE Assessments .....	3-1
3.2 Two Dosimeter EDE Assessments .....	3-3
3.3 Adjusted Single Dosimeter EDE Assessments .....	3-4
<b>4 EFFECTIVE DOSE EQUIVALENT IMPLEMENTATION RECOMMENDATIONS .....</b>	<b>4-1</b>
4.1 EDE Implementation Guidelines .....	4-1
A. For Routine Exposures .....	4-1
B. For Predominantly PA Exposures.....	4-2
C. For Exposures that Warrant a More Detailed Assessment of the EDE.....	4-2
<b>5 REFERENCES .....</b>	<b>5-1</b>
<b>A DETERMINING EFFECTIVE DOSE EQUIVALENT FOR EXTERNAL PHOTON RADIATION: ASSESSING EFFECTIVE DOSE EQUIVALENT FROM PERSONAL DOSIMETER READINGS.....</b>	<b>A-1</b>
By W. D. Reece and X. G. Xu.....	A-1



# LIST OF TABLES

---

Table 2-1 Organ Dose Weighting Factors.....	2-2
Table 3-1 Predicted EDE from a Single Front Badge Reading Divided by Actual EDE .....	3-2
Table 3-2 EDE and Front and Back Dosimeter Responses for Beam Exposures.....	3-2

# 1

## INTRODUCTION

---

Revisions effective in 1994 to Title 10 Part 20 of the Code of Federal Regulations require licensees to evaluate worker radiation exposure using a risk-based methodology termed *effective dose equivalent* (EDE or  $H_E$ ). EDE takes into account the variations in sensitivity to radiation of particular organs of the body by assigning radiation effects weighting factors to them, and then summing the weighted radiation exposures over certain organs and tissues. The resulting value is a measure of radiation dose that is proportional to the estimated risk.

This document provides EDE implementation guidelines to nuclear industry personnel. In particular, it explains how to accurately determine a worker's external EDE from radiation exposure measured by his or her dosimeter(s). These EDE assessments are valid for a very broad range of photon radiation sources (x-rays and gamma rays) and nuclear power plant exposure situations.

The EDE methodology described is based on research conducted by the Electric Power Research Institute (Palo Alto, CA).<sup>1,2,3</sup> The criteria for applying the methodology are presented, and the algorithms that can be applied to dosimeter measurements to yield the EDE are explained. Limitations or restrictions on the methodology are clearly stated.

Adopting this EDE methodology will support more effective personnel monitoring through:

- less conservative assessment of dose from radiation exposure
- eliminating the practice of using multiple dosimeters to account for non-uniform radiation fields
- limiting the practice of repositioning dosimeters on the body based on the radiation source location
- providing a technically sound basis for optimizing worker protection practices

# 2

## BACKGROUND

---

This section reviews the origin of EDE, describes the current way EDE regulations are implemented, and summarizes the EPRI EDE research program and results.

### 2.1 Origin and Basis of Effective Dose Equivalent

The concept of risk-based dose limits was introduced in a 1977 publication by the International Commission on Radiological Protection (ICRP).<sup>4</sup> The ICRP recommended that exposure limits for stochastic effects be based on the sum of the risks to individual organs (or tissues) of the body. They also specified the weighting factors to be applied to individual organ doses to account for differences in cellular radio-sensitivity, variations in susceptibility to stochastic effects, and variations in the treatability and lethality of different cancers. This approach has the advantage that as radiation effects knowledge improves, weighting factors can be periodically updated.

The ICRP recommendations for organ and tissue weighting factors (see Table 1) were adopted when the radiation protection standards of 10 CFR 20 were revised in 1991.<sup>5</sup> The revised regulations require that total effective dose equivalent be calculated by summing the external and internal components. The external component (herein called effective dose equivalent or EDE) is from radiation sources external to the body. The internal component (called committed effective dose equivalent) is from radiation ingested, absorbed, or respired.

**Table 2-1**  
**Organ Dose Weighting Factors**

Organ or Tissue	Weighting Factor
Gonads	0.25
Breast	0.15
Lung	0.12
Red Bone Marrow	0.12
Thyroid	0.03
Bone Surfaces	0.03
Remainder	0.30

## 2.2 Current Regulatory Framework

As noted above, the Nuclear Regulatory Commission (NRC) incorporated the effective dose equivalent concept as part of the 1991 revision to 10 CFR Part 20. In promulgating these standards, the NRC stated "the revision conforms to the Presidential Radiation Protection Guidance to Federal Agencies for Occupational Exposure and to recommendations of national and international radiation protection organizations" (i.e., the NCRP and ICRP). The Presidential Guidance<sup>6</sup> (issued in 1987) adopted the effective dose equivalent as reflected in ICRP Publication 26 and subsequent ICRP publications.

The revised standards define *effective dose equivalent* ( $H_E$ ) as "the sum of the products of the *dose equivalent* to the organ or tissue ( $H_T$ ) and the weighting factors ( $W_T$ ) applicable to each of the body organs or tissues that are irradiated." The standards include the table of *organ dose weighting factors* ( $W_T$ ) to be used in assessing the effective dose equivalent. (These organ dose weighting factors are the same as in Table 1 above.) Presently, use of the weighting factors is restricted to internal doses only. In the standards a single weighting factor of 1.0 is listed for external exposures of the whole body.

---

\* The "Remainder" category groups the other organs of the body, excluding the skin and the lens of the eye. The five organs in this category that receive the highest radiation exposure are each assigned a weighting factor of 0.06. The radiation exposures to the other remainder organs and tissues give rise to trivial risk, and—by convention—are neglected.

In the Supplementary Information<sup>7</sup> issued with the revision to Part 20, the NRC noted that a number of public comments had been received requesting that licensees be permitted to use risk-based organ dose factors in assessing the effective dose equivalent for external exposures. However, at the time of rule issuance, none of the principal standard-setting organizations had published specific recommendations for the use of weighting factors for external dose. Therefore, the NRC specified only a single weighting factor,  $W_T = 1.0$ , to be used for external doses to the whole body, including the head, trunk, arms above the elbow, or legs above the knee.

The NRC recognized there were ongoing efforts to develop methods for calculating specific organ doses from external radiation exposure, and the “practical problems” that might be associated with such methods. The NRC provided for the use by licensees of other weighting factors for external exposure, to be approved on a case-by-case basis upon request to the NRC. This provision is described in footnote 2 to the table of organ dose weighting factors ( $W_T$ ) in the regulations. This technical guideline, along with the referenced EPRI technical reports can serve as the basis for obtaining approval from the NRC for use in demonstrating compliance with 10 CFR Part 20.

In the revised Part 20, NRC established an annual occupational radiation dose limit of 5 rem (0.05 Sv) total effective dose equivalent. The *total effective dose equivalent* (TEDE) is defined as “the sum of the deep-dose equivalent (for external exposures) and the committed effective dose equivalent (for internal exposures).” The standards define the *deep-dose equivalent* ( $H_d$ ), as “the dose equivalent at a tissue depth of 1 cm (1,000 mg/cm<sup>2</sup>).” Further, the revised Part 20 requires that “the assigned deep-dose equivalent ... must be for the part of the body receiving the highest exposure” (§20.1201). Consequently, the revised Part 20, does not currently support licensee implementation of the effective dose equivalent for external exposures.

In response to a proposed rulemaking to Part 20, the Nuclear Energy Institute has recommended that the NRC revise the definition of total effective dose equivalent with the objective of facilitating licensee implementation of the effective dose equivalent for external exposures.

## 2.3 Research Summary

The paragraphs immediately following briefly summarize the EPRI research. Appendix 1 describes the research in detail. It is important to note that the existing method of assessing external effective dose equivalent (a single front-worn dosimeter) is adequate and conservative.

The research was conducted in two phases. In the first phase, the effective dose equivalent was calculated for a very large number of beam and point radiation sources emitting single-energy photons. Three photon energies were used (80 keV, 300 keV, and 1.0 MeV), a range that spans the energies commonly encountered in nuclear power plants. Mathematical models (phantoms) of the adult male and female were taken from the literature. All of the significant organs and tissues are described in these models and are appropriately assigned as one of three tissue types: bone, lung, or soft tissue. For each of the individual beam and point sources, a well-known and widely-accepted Monte Carlo radiation transport code was used to calculate the behavior of individual photons emitted by that source, and tally energy deposition at numerous places within the phantoms. From this, the computer code was used to determine the dose deposited in each organ or tissue, then the organ weighting factors<sup>\*</sup> were applied to those doses, and finally the doses were summed to give the external effective dose equivalent (per unit fluence) for that exposure. Tabular and graphical summaries of EDE were produced for 1) beams striking the body from any orientation, and 2) point sources on, and at various distances from, the body (see Appendix 1). These results show how radiation striking the body from any direction interacts with the body's organs and tissues.

The second phase of this study related EDE to dosimetry. Dosimetry is a measure of total photon energy fluence at a discrete location on the surface of the body. Accordingly, small, air-filled spheres, each with a radius of 1 cm, were modeled at 480 different locations on the surface of a composite (male/female) phantom. Monte Carlo simulations using the phantom were done for broad parallel photon beams of various energies and for isotropic point sources. The code was used to tally the number of photons incident on or backscattered into each sphere, as well as the path length of each photon contained within the spherical volume. These results demonstrate how surface photon energy fluence (which can be correlated to dosimeter response) varies at different locations on the body for a given exposure. The results are presented in reference 2 as contour plots of normalized dosimeter response on the surface of the body. These data were used to determine locations for optimum dosimeter placement.

---

<sup>\*</sup> Some of the organ weighting factors are different for males and females. For a 50% male / 50% female population the weighting factors reduce to the ICRP values shown in Table 1.

The research resulted in the following conclusions:

### ***Beam Sources***

- For equivalent energy fluxes, lower energy photons produce lower effective dose equivalents.
- Beams striking the torso from the front (anterior-posterior or AP) produce the highest EDE per unit fluence.
- Beams striking the torso from the rear (posterior-anterior or PA) produce the second highest EDE per unit fluence.
- Effective dose equivalent decreases significantly as one departs from the AP or PA orientation.
- Females have higher EDE per unit fluence than males for all photon energies and all beam angles.

### ***Point Sources in Contact With the Torso***

- For females the highest EDE occurs when the point source is on the front of the torso near the sternum.
- For males the highest EDE occurs when the source is on the front of the torso near the gonads.
- The EDE from a point source on the male gonads is higher than the EDE from an identical source on the sternum of the female.
- For all other point source locations, the female has a higher EDE per unit exposure than the male.

### ***Point Sources Away From the Torso***

- Because flux from a point source decreases as the reciprocal of the distance from the source squared, point sources on the torso expose only those organs and tissues that are quite close to the source.
- Effective dose equivalent drops dramatically for point sources a foot or more away from the torso, compared to the same sources in contact with the torso.

### **Surface Flux Measurements (Dosimeter Simulations)**

- Isotropic dosimeters that are directly exposed by a beam all read essentially the same, regardless of their location on the torso. For example, for beams striking the torso from the front, dosimeters worn on the forehead, thorax, abdomen, or front of the upper legs, will show essentially the same readings. The small differences in readings result from variations in photon backscatter. Most backscattered photons have low energies, meaning their contribution to the dosimeter response is small.
- The effective dose equivalent resulting from exposure to an overhead beam (both near or directly overhead) is much lower than the equivalent AP exposure, due to self-shielding by the body and other factors. A dosimeter placed on the head overestimates EDE from a source directly overhead by a factor of three to seven, depending on photon energy. The same is true of underfoot exposures.
- For front, back, or side beam exposures, dosimeters shielded by the body (shadowed) will under-respond by up to 90% at low energies (80 keV) and 50% at high energies (1.0 MeV). For beam sources **near** overhead or **near** underfoot, the under-response can be even greater because of the large slant distances through the body. (An example of a shadowed dosimeter responding to a near overhead beam source would be a chest-worn dosimeter and a source behind and above the body.)

# 3

## EFFECTIVE DOSE EQUIVALENT METHODOLOGY

---

This section describes methods for accurately assessing external effective dose equivalent using measurements from either one or two dosimeters worn on the body (typically attached to the outside of protective clothing). In addition, ways to more accurately assess EDE and avoid large overestimates from certain single dosimeter assessments, are discussed.

Dosimetry measurements are complex, and there are many factors related to the radiation source, dosimeter construction, and dosimeter readout process that can result in measurement variations and uncertainties. Accordingly, it is appropriate to understand what constitutes acceptable dosimeter measurement accuracy. The International Commission on Radiological Protection has recommended<sup>8</sup> a factor of 1.5 or less at the 95% confidence level for exposures near the maximum permissible levels of 50 mSv (5 rem), or a factor of 2 or less at the 95% confidence level when the annual reported dose is less than 10 mSv (1 rem). Since the vast majority of nuclear power plant exposures are < 10 mSv, being within a factor of two of the effective dose equivalent is considered acceptable performance.

### 3.1 Single Dosimeter EDE Assessments

For routine exposures, dosimeters calibrated for AP exposures and worn on the front of the body will yield conservative EDE values. By routine exposures we mean those characteristic of typical power plant work, where a worker is moving relative to a number of radiation sources, so that photons strike the body from many different angles. Isotropic or rotational geometries can be used as a model for such exposures. Isotropic sources are those in which photons appear uniformly from all directions. Rotational geometry is defined as beams of photons uniformly distributed about all azimuthal angles. Alternately, rotational geometry can be defined as the dose arising from a worker rotating at a uniform rate in a beam of photons. As shown in the table below, EDE is adequately assessed by a single dosimeter worn on the front of the torso, even though half of the exposure comes from the rear.

**Table 3-1****Predicted EDE from a Single Front Badge Reading Divided by Actual EDE**

	Photon Energy		
	80 keV	300 keV	1 MeV
Rotational	0.87	1.04	1.03
Isotropic	1.06	1.26	1.19

Consider the case in which a worker is exposed to only AP or PA beams. Table 3 shows the EDE, along with the readings that would be seen for isotropic dosimeters worn on the front and back.

**Table 3-2****EDE and Front and Back Dosimeter Responses for Beam Exposures**

	80 keV Photons			300 keV Photons			1 MeV Photons		
	EDE	Front	Back	EDE	Front	Back	EDE	Front	Back
AP	0.48	0.55	0.06	1.60	2.01	0.51	4.56	5.58	2.30
PA	0.40	0.07	0.53	1.30	0.51	1.99	4.05	2.29	5.56

By taking simple ratios from the data in Table 3, we see that for the front dosimeter to under-predict EDE by 30% (a error much less than the factor of two deemed acceptable by the ICRP) the source would have to come from the rear:

- 46% of the time for 80 keV photons
- 64% of the time for 300 keV photons
- 80% of the time for 1 MeV photons.

These figures are "worst case" scenarios for beams. If the front exposure departs from AP or the back exposure departs from PA, the fraction of posterior exposure necessary to lower front badge response to 70% of the true EDE will rise. This is because even modest departures from AP or PA exposures will greatly decrease EDE. Thus, for lateral, overhead, or underfoot sources, even more of the exposure would have to be posterior for the isotropic front-worn badge to under-predict EDE by even 30%.

Since much advance planning goes into work in high radiation fields, radiation protection personnel are generally in a position to know how a worker will be

positioned relative to the radiation sources. If these assessments indicate a highly dominant PA source, then repositioning the single dosimeter to the worker's back will yield an accurate EDE measurement. Otherwise, wearing the dosimeter on the front is accurate and conservative.

### 3.2 Two Dosimeter EDE Assessments

Less conservative EDE assessments will be obtained by wearing two dosimeters, one on the front and one on the back, and applying an algorithm to their readings. For routine exposures, such use of two dosimeters would typically result in reported doses 10-20% less than with a single, front-worn badge. This improvement in accuracy via reduced conservatism may not be justified by the costs of handling and processing extra dosimeters. However, for high dose or complex exposures, using two dosimeters may prove cost-effective.

The EPRI research program found that two two-badge algorithms gave satisfactory EDE assessments:

1. An algorithm that averages the chest dosimeter and back dosimeter readings.

$$H_E = \text{Avg} (R_{\text{Front}} + R_{\text{Back}}) = \frac{R_{\text{Front}} + R_{\text{Back}}}{2}$$

2. An algorithm that weights the higher reading.

$$H_E = \frac{\text{Max} (R_{\text{Front}} \text{ or } R_{\text{Back}}) + \text{Avg} (R_{\text{Front}} + R_{\text{Back}})}{2}$$

where:

$R_{\text{Front}}$  = the reading from the front-worn dosimeter

$R_{\text{Back}}$  = the reading from the back-worn dosimeter

Avg = the average of the front and back dosimeter readings

Max = the higher of the front or back dosimeter readings.

The algorithm that yields an EDE that is closest to the "true" EDE (as calculated by the Monte Carlo method) depends upon the exposure conditions. The calculations showed the weighted algorithm did slightly better with AP or PA exposures. In addition to the calculations, laboratory and nuclear power plant field experiments were conducted in which tissue equivalent physical phantoms—imbedded with 50-200 thermoluminescent

dosimeter packets—were exposed to various radiation fields. In these experiments, the averaging algorithm performed slightly better in predicting the measured dose. In those radiation exposure situations where licensees choose to use two dosimeters, either algorithm may be used with confidence. Both will yield an effective dose equivalent that is numerically lower than that yielded by a single dosimeter.

### **3.3 Adjusted Single Dosimeter EDE Assessments**

As stated above, a single dosimeter worn on the front of the body results in generally conservative measurements of dose. For typical exposures (i.e., other than PA exposures) such single-dosimeter monitoring will over-estimate EDE by 5-20%, depending on photon energy and source geometry. Such differences are well within the errors associated with dosimeter calibration and dose measurement. Accordingly, it is generally not appropriate to adjust single badge readings to produce less conservative EDEs.

However, under some exposure circumstances the overestimation can be substantially larger. For overhead or underfoot sources for example, the front-worn badge over-predicts EDE by a factor of 2-4. Therefore, there may be circumstances where adjusting a single badge reading may be appropriate. For example, an adjustment of a single-badge reading may be appropriate as part of an investigation of an unplanned exposure, to more accurately assess the significance and consequences. In these circumstances it is common to reconstruct the event by analyzing the radiation field and the worker's movements within the field.

Because the range of potential exposure circumstances is so great, it is impractical to identify a single-dosimeter correction factor. Nonetheless, corrections can still readily be made once exposure geometries are reconstructed. If the reconstructed exposure geometry is anterior (AP beam), posterior (PA beam), or from the side (lateral beam), then the correction factors can be taken directly from the tables in reference 2 (interpolating as necessary to account for photon energy).

As the radiation incidence angle departs from AP, EDE declines. Commercial dosimeters are also non-isotropic, that is they show directional dependence. For most commercial dosimeters, EDE falls more quickly than the badge response, thus the badge remains conservative. Tables showing the angular response of EDE versus beam angle<sup>9</sup> may be used to correct single badge readings. (It is important to remember that any corrections made to single badge readings cannot be used in the two-badge algorithms discussed above; these two-badge algorithms must use uncorrected readings.)

# 4

## EFFECTIVE DOSE EQUIVALENT IMPLEMENTATION RECOMMENDATIONS

---

The EPRI research has shown that the current practice of using a single, front-worn dosimeter for routine power plant exposures is conservative. In addition, the research has shown that for exposures in which the vast preponderance of photons will strike the body from either the front hemisphere or the rear hemisphere, accurate EDE can be assessed simply by placing the dosimeter on the front or the back of the torso. Finally, the research has shown that even in exposure situations involving highly directional sources or sources of unknown geometry, two dosimeters (one front-worn and one back-worn) are all that are needed to accurately assess EDE.

### 4.1 EDE Implementation Guidelines

Licensees may choose to factor these basic findings into their dosimetry practices. One way of doing so is presented below. The guidelines below are not intended to be prescriptive. Each licensee should assess their dosimetry practices against the EPRI research results, and determine whether revisions are warranted. Licensees should remain alert for special circumstances—eye exposure, working behind a shadow shield, etc.—that may justify special dosimetry or special dosimetry placement.

#### **A. For Routine Exposures**

(Defined as a radiation exposure situation where a worker is moving relative to a number of radiation sources, so that photons strike his or her body from many different angles. These are typical exposures for nuclear power plant work.)

1. Use a single dosimeter worn on the front of the torso. Use the measured radiation exposure from that dosimeter as the reported effective dose equivalent for the worker.
2. Two dosimeters (front and back) may be used, though this is not necessary for an accurate EDE assessment.

3. It is not necessary to place many dosimeters on workers or reposition their single dosimeter in an attempt to account for non-AP incident radiation.

***B. For Predominantly PA Exposures***

(Defined as radiation exposure situations where the vast preponderance of the exposure for a task is expected to come from behind a worker.)

1. Reposition the worker's single dosimeter to the rear of the torso. Use the measured radiation exposure from that dosimeter as the reported effective dose equivalent for the worker.
2. Two dosimeters (front and back) may be used, though this is not necessary for an accurate EDE assessment.

***C. For Exposures that Warrant a More Detailed Assessment of the EDE***

(Defined as potentially high-exposure situations, or where the radiation sources' exposure geometries are complex and the expected worker dose is difficult to estimate, or where the licensee otherwise chooses to reduce the conservatism in reported exposures.)

1. Consider using two dosimeters, one worn on the front of the torso and one on the back.
2. If two dosimeters are used, select one of the two-dosimeter algorithms discussed in this document and apply it to the two dosimeter readings to calculate the effective dose equivalent.
3. It is not necessary to place many dosimeters on workers or to reposition dosimeters to face known radiation sources.
4. Develop procedures or guidelines for adjusting the measured reading from a single dosimeter if necessary. Such adjustments should be based on specific characteristics of the radiation field and exposure reconstruction, and on the effects of the angle of incident radiation on both the effective dose equivalent and the dosimeter response.

# 5

## REFERENCES

---

1. W.D. Reece, J.W. Poston, and X.G. Xu, "Assessment of the Effective Dose Equivalent for External Photon Radiation—Volume 1: Calculational Results for Beam and Point Geometries," Electric Power Research Institute, EPRI TR-101909, February 1993.
2. W.D. Reece, J.W. Poston, and X.G. Xu, "Assessment of the Effective Dose Equivalent for External Photon Radiation—Volume 2: Calculational Techniques for Estimating External Effective Dose Equivalent from Dosimeter Readings, EPRI TR-101909-V2, June 1995.
3. W.D. Reece and X.G. Xu, "Determining the Effective Dose Equivalent for External Photon Radiation: Predicting Effective Dose Equivalent from Personal Dosimeter Readings, *Radiation Protection Dosimetry*, Vol. 69, No. 3, pages 167-178, 1997.
4. International Commission on Radiological Protection, "Recommendations of the International Commission on Radiological Protection," ICRP Publication 26, *Annals of the ICRP*, Vol. 1 No. 3, Pergamon Press, 1977.
5. 10 CFR Part 20, "Standards for Protection Against Radiation," *Federal Register*, Vol. 56, page 23360, issued on May 21, 1991.
6. "Radiation Protection Guidance to Federal Agencies for Occupational Exposure," *Federal Register*, Vol. 52, No. 17, pages 2822-2834, January 27, 1987.
7. 10 CFR Part 20, op cit.
8. International Commission on Radiological Protection, "General Principles of Monitoring for Radiation Protection of Workers," ICRP Publication 35, Pergamon Press, Oxford, 1982.
9. X.G. Xu, W.D. Reece, J.W. Poston, "A Study of the Angular Response Problem in Effective Dose Equivalent Assessment," *Health Physics*, Vol. 68, No. 2, p.214-224, 1995.

# A

## **DETERMINING EFFECTIVE DOSE EQUIVALENT FOR EXTERNAL PHOTON RADIATION: ASSESSING EFFECTIVE DOSE EQUIVALENT FROM PERSONAL DOSIMETER READINGS**

---

**By**

**W. D. Reece and X. G. Xu**



Radiation Protection Dosimetry  
Vol. 69, No. 3, pp. 167-178 (1997)  
Nuclear Technology Publishing

## DETERMINING EFFECTIVE DOSE EQUIVALENT FOR EXTERNAL PHOTON RADIATION: ASSESSING EFFECTIVE DOSE EQUIVALENT FROM PERSONAL DOSEMETER READINGS

W. D. Reece and X. G. Xu\*  
Department of Nuclear Engineering  
Texas A&M University, Room 129, Zachry Bld  
College Station, Texas 77843-3133, USA

Received July 31 1995, in final revised form June 17 1996, Accepted November 14 1996

**Abstract**— Since January 1994, US nuclear plants have implemented Title of 10 Part 20 of the US Code of Federal Regulations which adopted the methodology of ICRP 26 for effective dose equivalent ( $H_E$ ) for internally deposited radionuclides. To provide general guidance for assessing  $H_E$  from external photon exposures, a two-phase research programme was performed. This article presents the results for the second phase — assessment of  $H_E$  using personal dosimeters. By using a Monte Carlo photon transport code, personal dosimetry was simulated at 480 different locations on the surface of a hermaphroditic phantom. The dosimeter readings were compared with  $H_E$  calculated for a variety of photon sources completed during the first phase of this study. The data suggest that the current one-badge approach is still valid in assessing  $H_E$  for routine exposure in many radiation fields and two dosimeters may be used for situations in which the exposure is less uniform. Algorithms to relate dosimeter readings to  $H_E$  are discussed for uniform and non-uniform exposures.

### INTRODUCTION

Since January 1994, US nuclear plants have implemented Title of 10 Part 20 of the US Code of Federal Regulations (10CFR20)<sup>(1)</sup> (*Standard for Protection Against Radiation*). The new regulations adopt the methodology of ICRP 26 for effective dose equivalent ( $H_E$ ) from internally deposited radionuclides<sup>(2)</sup>. For exposure to sources outside the body, however, the new regulations propose an *ad hoc* extension of the ICRP 26 methodology by defining a new tissue — 'the whole body' — and assigning it a weighting factor of one. To provide general guidance for assessing  $H_E$  from external photon exposures, a two-phase research project was undertaken. Results for the first phase of the research — calculations of organ doses and  $H_E$  for a variety of different exposure geometries — have been published earlier<sup>(3)</sup>. This article presents a brief summary of the results from the first efforts, followed by a discussion of the assessment of  $H_E$  using personal dosimeters.

### SUMMARY OF CALCULATIONS OF ORGAN DOSES AND $H_E$

During the first phase of this research<sup>(3)</sup> organ doses and  $H_E$  were calculated using the Monte Carlo computer code MCNP (Monte Carlo Neutron-Photon)<sup>(4)</sup> to simulate photon transport through anthropomorphic

phantoms (mathematical models of the human body). In this approach, the human body was mathematically modelled and the behaviour of a very large number of incident photons striking the body was calculated. The mathematical models used were those developed by Cristy and Eckerman<sup>(5)</sup>, representing a standard adult male and female. Each phantom consists of three major sections:

- (i) the trunk and arms (represented by an elliptical cylinder);
- (ii) the legs and feet (represented by two truncated circular cones);
- (iii) the head and neck (represented by an elliptical cylinder capped by half an ellipsoid).

The various organs within these sections were modelled geometrically and assigned one of three tissues: skeletal, lung, or soft tissue. The models consist of a large number of equations, each describing a particular anatomical feature of the phantom. Additional details on the phantoms and descriptions of how the MCNP code was run and how the data were processed are available<sup>(6)</sup>.

### Results for beam sources

Beams, which irradiate uniformly across the height of the torso, are commonly encountered radiation sources that are easy to understand and characterise. Since all finite sources behave as beam sources as the distance between the source and the receptor increases, if beam sources are understood, then we also understand

\* Current Address: Department of Nuclear Engineering and Engineering Physics, Rensselaer Polytechnic Institute, N. Bld., Tibbits Ave, Troy, New York 12180-3590, USA.

the limiting case for all other finite sources. In this investigation, monoenergetic photons of 0.08, 0.3, and 1.0 MeV were studied. To specify the direction of the beams, a polar-azimuthal coordinate system was used. The angles considered in this study were azimuthal angles at 0°, 45°, 75°, 90°, 105°, 135°, 180°, 225°, 255°, 270°, 285°, 315°, 360°, and polar angles at 0°, 15°, 45°, 90°, 135°, 165°, 180°. This provided sufficient detail so that simple interpolation through any two adjacent angles would be equal or less than the 4% error inherent in the MCNP calculations. Among these beam directions, parallel beams striking the torso from the front to the back at right angles to the long axis of the body are termed anterior-posterior beams (abbreviated AP). Conversely, parallel beams striking the torso from the back to the front are termed posterior-anterior beams (abbreviated PA). And beams striking the torso from either side are termed lateral beams (abbreviated LAT).

Results for beam sources indicate that beams striking the torso normal to the body's major axis produce the largest  $H_E$ . For all photon energies considered,  $H_E$  is higher for the beams striking the front of the torso than it is for beams striking the rear of the torso. For the same beam direction and energy, females are shown to have higher  $H_E$  than males.  $H_E$  falls dramatically as one moves from the AP or PA orientations. Although concern has been expressed in the literature about underfoot and overhead sources, the  $H_E$  drops markedly for these sources. Questions are often raised as to the adequacy of radiation workers' dosimetry, in particular whether or not their dosimetry is at or near the point of highest exposure on the torso. Indeed, the US Nuclear Regulatory Commission (USNRC) has levied civil penalties against some utilities for not having dosimeters at the point of highest dose<sup>(7,8)</sup>. This concern has led to the widespread practice of multi-badging radiation workers and assigning the highest dose among the multiple dosimeters as the dose of record<sup>(9)</sup>. The results obtained in the first phase of the research show that practice to be overly conservative. As the angle of beam incidence is changed from AP,  $H_E$  drops dramatically. The drop-off is often more than the under-response of a dosimeter, thus dosimeters will not under-predict  $H_E$  regardless of the incident photon angles<sup>(10)</sup>. Moreover, dosimeters worn at the points of highest dose on the surface over-respond, since they are calibrated for AP exposures that produce the highest effective dose equivalent per unit fluence. The beam data also demonstrate that dose assessment methodologies for external photons can be based on fully developed anthropomorphic phantoms rather than on the simple slabs, cylinders, or spheres as is the current practice. This should help end overly conservative exposure estimates, and begin the process of assigning radiation doses that realistically estimate the risk of radiation injury.

The results from the first phase of this research allow understanding of how radiation striking the body from any direction or distance interacts with various organs

and tissues. By knowing the mean absorbed dose to all the organs and tissues, the weighted dose to the organs and  $H_E$  can be calculated. To make practical use of the  $H_E$  calculations, however, additional data are needed. The dose to a worker's organs cannot be monitored directly, nor can the energy, geometry, and exposure times of all the sources be known exactly. Each worker will only have radiation dose assigned as measured by the external dosimeters he/she wears. The challenge is to relate those few measurements to the actual  $H_E$  received by the worker with some degree of confidence. One should note that the quantity measured by a dosimeter differs from  $H_E$  on which regulatory limits are based. Knowing that the response of personal dosimeters is influenced by, among other factors, the positioning of dosimeter and orientation of the body in the radiation field (e.g. a dosimeter may be shielded by the body and, therefore, does not directly register radiations from the source), the task of relating dosimeter indications to  $H_E$  is not trivial. Analysis of some of the problems in assessing effective dose equivalent from dosimeter readings have been published previously. A partial review is given in NCRP Publication 129<sup>(11)</sup>. The first step to relate dosimeter readings to  $H_E$  is determining how dosimeter readings vary as a function of location on the surface of the body for various exposure geometries.

#### PERSONAL DOSEMETER SIMULATIONS

A personal dosimeter carried by an individual provides a reading that, with proper calibration, is used as the dose of record for the wearer. One of the goals in this research was to study the effects of dosimeter position on the body on dosimeter response as a function of photon energy. The results of this study help provide a basis for the development of algorithms that can be used to interpret dosimeter readings to assess  $H_E$ . To investigate the effect of dosimeter placement, personal dosimeters were simulated at 480 locations over the surface of the phantom. A simplified adult hermaphroditic phantom which has only the skeleton, tissue, and lungs, was adequate since dose to organs was not needed for this part of the study.

In general, dosimeter readings can be related directly to photon energy fluences at the surface of the phantom including the incident and scattered photons at the interface between the phantom and the surrounding air. To simulate radiation transport through a dosimeter, the size, geometric shape, and material of the dosimeter need to be considered. Many researchers have simulated radiation response of dosimeters using Monte Carlo computer codes<sup>(12,13)</sup>. Usually, a dosimeter was modelled using tissue-equivalent material and a simple shape such as a sphere or a cube. Unfortunately, only one or a few dosimeter positions can be considered by this method and many histories must be calculated because of the small target size a dosimeter presents.

# $H_E$ FROM PERSONAL DOSEMETERS

Dosimeter simulations were performed differently in our study. Small air-filled spheres, each with a radius of 1 cm, were defined at 480 locations on the surface of the phantom including the head, torso, left upper leg, and right upper leg. The Cristy-Eckerman phantoms, by convention, express position along the long axis of the body as Z-axis values, with the juncture of the torso and legs of the phantom being where  $Z = 0$  cm. The Z-axis values for each portion of the phantom are as follows:

head:  $Z = 71$  to  $91$  cm  
torso:  $Z = 1$  to  $66$  cm  
upper legs:  $Z = -49$  to  $-4$  cm.

Figure 1 shows the cross sections of these air spheres on the surface of the torso at height  $Z = 41$  cm (the chest region of the phantom). Dosimeter locations are close enough together that dosimeter responses can be plotted on the phantom's surface using contour lines. A complete list of all the dosimeter locations can be found in Xu<sup>(6)</sup>. These positions were selected not only to account for the most common dosimeter positions found in regular operations, but also in special operations during which dosimeters may be placed on top of the head, on the upper legs, or on the back of the body<sup>(7,8)</sup>.

Because MCNP allows only 100 tallies in each calculation, five separate computer runs were needed to complete the 'mapping' of the total 480 dosimeter positions for a given irradiation geometry and energy. Furthermore, due to the small volume of the air-filled spheres, each computer run to calculate dosimeter readings took longer than for the corresponding  $H_E$  calculations for the same statistical uncertainty. For the dosimeter response computer runs, photon transport and energy depositions in the air-filled spheres were tallied in MCNP and the

energy fluences were calculated by track length estimates for each sphere. These track length estimates are quite reliable because there are usually many tracks in each sphere. The contribution from many separate tracks to the tally reduces the statistical uncertainty compared to other direct energy deposition tally methods. Photon energy fluences at each energy were multiplied by mass energy absorption coefficients for dosimeter materials of interest to find dosimeter readings. That is, assuming charged particle equilibrium (CPE) exists, absorbed dose,  $D$ , to a small volume will be equal to the collision kerma,  $K_c$ , which is related to energy fluence  $\Psi_E$  by the mass energy absorption coefficient,  $\mu_{en}/\rho$ , i.e.<sup>(14)</sup>

$$D = K_c = \int_{E=0}^{E_{\max}} \Psi_E(E) \left( \frac{\mu_{en}}{\rho} \right) dE \quad (1)$$

where, the CPE above the equality sign emphasises its dependence upon that condition,  $\Psi_E(E)$  is the differential distribution of photon energy fluence,  $\mu_{en}$  is the linear energy absorption coefficient which is characteristic of the photon energy  $E$  and the atomic number  $Z$  of the physical dosimeter material, and  $\rho$  is the density.  $E_{\max}$  is the maximum photon energy, equal to the photon source energy.

Collision kerma calculated in this way would equal the dose in (or reading from) a real dosimeter worn at the same location on the body, provided that CPE or transient charged particle equilibrium (TCPE) exists and the attenuation by the dosimeter capsule is negligibly small. CPE or TCPE is achieved in dosimetry packages by using build-up material of appropriate thickness. For simplicity, the term 'dosimeter reading' will be used hereafter, rather than collision kerma or dosimeter response.

In MCNP, energy fluences within each air-filled sphere were calculated with energy bins having upper limits of 0.01, 0.02, 0.03, 0.04, 0.05, 0.06, 0.08, 0.10, 0.15, 0.20, 0.30, 0.40, 0.50, 0.60, 0.80, 1.0 MeV. The integration in Equation 1 was carried out by summing over each term associated with these energy bins. Post-processing codes were developed to extract energy fluence data from each run and mass energy absorption coefficients for different materials (provided by Hubbell<sup>(15)</sup> and tabulated by Attix<sup>(14)</sup>) were multiplied by the photon energy fluence in the energy bin.

This approach of using air-filled spheres to calculate energy fluences and then multiplying the energy fluences by the mass energy absorption coefficients to find dosimeter readings has several advantages over direct simulation of a dosimeter:

- (1) More than one dosimeter material can be considered easily. The dosimeter material in which we were most interested was the ICRU tissue-equivalent material<sup>(16)</sup>. Other materials, such as LiF, were also considered for comparison.
- (2) A large number of dosimeter locations can be

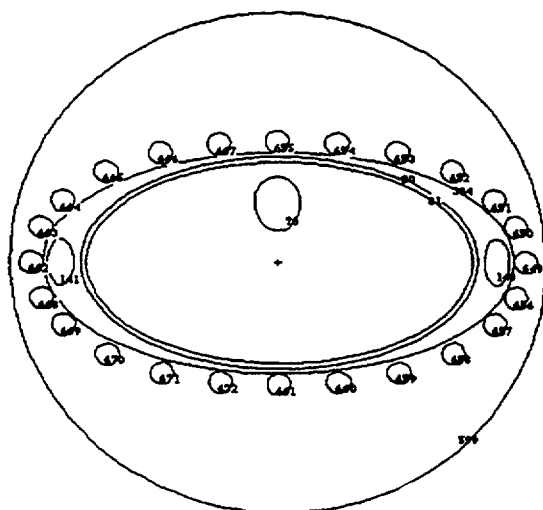


Figure 1. Cross section of phantom at  $Z = 41$  cm showing small air spheres on the surface of the phantom to simulate dosimeters.

W. D. REECE and X. G. XU

- studied in the same MCNP run without the photon field being disrupted by the other dosimeters.
- (3) The details of an actual dosimeter's construction can be neglected if TCPE is achieved.

Broad parallel photon beams was the first geometry used with the simplified mathematical phantom and the small air-filled spherical dosimeters. For photon beam sources, irradiation geometries AP, PA, LAT, overhead, and underfoot were selected to calculate surface energy fluences and dosimeter readings to study the effect of dosimeter position and to test algorithms designed to evaluate  $H_E$ . Our earlier<sup>(3)</sup> results show that these geometries bound many exposure situations encountered in the workplace. Another geometry with photon beams incident from 45° azimuthal and 45° polar angles was used to represent a more or less arbitrary exposure geometry. The geometries studied for dosimeter positioning and algorithm development are only a fraction of the geometries used for  $H_E$  calculations. Nonetheless, the data are sufficient to be applicable to general cases. Because the relationships between  $H_E$  and source geometry are well understood, only a few representative geometries are necessary to establish general cases.

#### Results for dosimeter positioning studies

As with phase 1 of this effort, monoenergetic photons of 0.08, 0.3, and 1.0 MeV were used in this study. The

large number of dosimeters, variety of photon energies, and numerous geometries involved make the results for dosimeter simulations unwieldy to present in tabular form. Whole-body contour plots illustrate more efficiently how dosimeter position on the body influences the reading. Figures 2 through 9 are contour plots for dosimeter readings for different source geometries and energies. Smooth contour lines were drawn among data obtained at the 480 different dosimeter positions on the surface of the body using spline interpolations among the data points. On each plot, the phantom surface is divided into four different portions: head, torso, upper left leg, and upper right leg. Each portion is cut from the back and flattened to show, in a two-dimensional area, the dosimeter reading as function of location. Each location on the phantom is defined by height along the Z axis and distance around the body horizontally (starting at the back, continuing along the right side to the front, and continuing around the left side and terminating at the back). Minor distortions are allowed in drawing the horizontal axis in terms of relative locations such as, 'back', 'right', 'front' and 'left', particularly for legs which were defined as cones in the phantoms but treated as cylinders when plotting. The dosimeter reading located at centre-of-chest ( $Z = 41$  cm) was used to normalise the results. This reference value is given in the caption of each plot in the units of

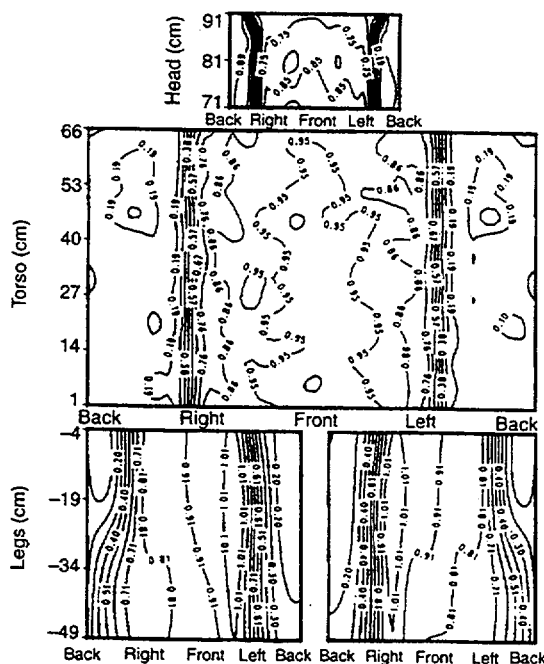


Figure 2. Contour plot for normalised dosimeter response exposed to 0.08 MeV AP beam source for different dosimeter locations on the head, torso, and upper legs. Reference value,  $0.55 \times 10^{-12}$ .

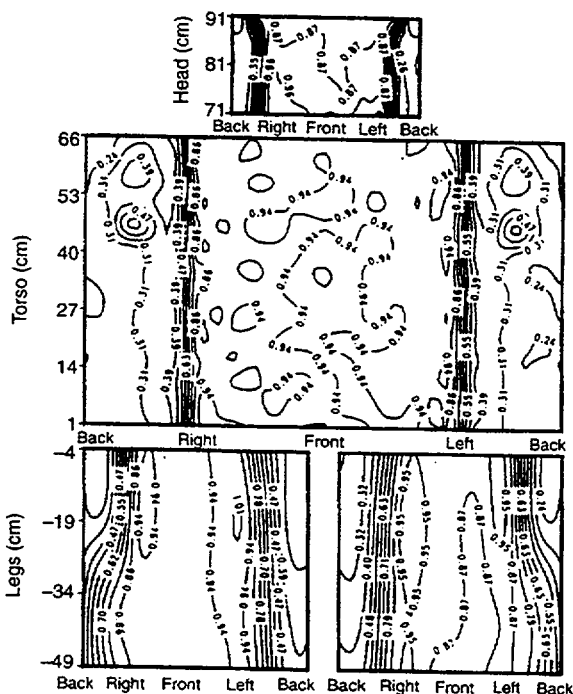


Figure 3. Contour plots for normalised dosimeter response exposed to 0.30 MeV AP beam source for different dosimeter locations on the head, torso, and upper legs. Reference value,  $2.01 \times 10^{-12}$ .

# $H_E$ FROM PERSONAL DOSEMETERS

Sv per photon fluence ( $\text{Sv}\cdot\text{cm}^{-2}$ ). The data shown by the contour lines are the relative to the reference dosimeter. The absolute dosimeter readings can be found by multiplying these relative readings by the reference dosimeter reading.

## Parallel photon beam exposure — AP

Results for this source geometry are shown in Figures 2, 3, and 4, for 0.08, 0.3, and 1.0 MeV photons, respectively. For this geometry, the dosimeter readings for dosimeters facing the radiation source (those dosimeters that are located in region marked from 'right' to 'front' and then to 'left') range from 0.85 to 1, from 0.88 to 1, and from 0.92 to 1, for 0.08, 0.3, and 1.0 MeV photon beams, respectively. For dosimeters located near the centre of the chest area, dosimeter readings are all nearly equal; they differ little from the reference dosimeter. Since the incident fluence is the same for all dosimeters placed on the front side of the body for AP exposures, the differences in dosimeter readings arise solely from different backscattered fluence contributions at each location on the surface of the body. Most of the backscattered photons are low energy and their contribution to dosimeter reading is small. Our results suggest that for whole-body AP exposure, perhaps the most common exposure encountered in the workplace, a specific requirement on dosimeter location is not necessary,

provided that the dosimeter is directly exposed to the source. For the AP geometry, and other nearly AP geometries, dosimeters worn on the forehead, or thorax, or abdomen, or front side of the upper legs, will have almost the same readings.

However, dosimeters worn on the back of the torso are shielded by the body for AP exposure geometry. Located within the regions from 'back' to 'right' and from 'left' to 'back' in Figures 2, 3, and 4, these dosimeters show larger variations in reading among themselves depending on the photon source energy and the specific location on the back. The relative readings for these dosimeters range from approximately 0.1 to 0.75, from 0.25 to 0.8, and from 0.45 to 0.85, for 0.08, 0.3, and 1.0 MeV photon beams, respectively. As is evident from these contour plots, the large variations in response among these dosimeters are caused by the differing densities of body components. Tissues, such as the lungs, allow more photons to penetrate the body, while bones cause the photons to be attenuated and backscattered. As would be expected, the maximum difference in response among these dosimeters is greater for less penetrating photon beams.

Because of the attenuation in the body, dosimeter readings on the back of the torso are smaller than those placed on the front of the body for AP geometry. The relative dosimeter readings for a dosimeter located on the back of the body at a height  $Z = 41$  cm to that for

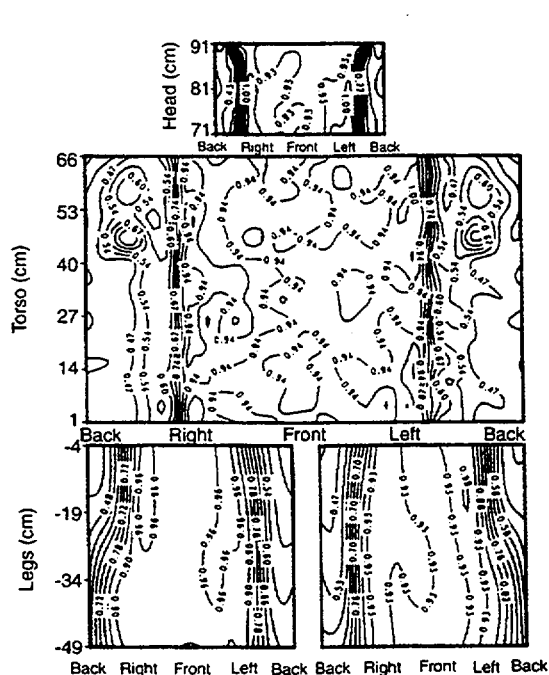


Figure 4. Contour plot for normalised dosimeter response exposed to 1.0 MeV AP beam source for different dosimeter locations on the head, torso, and upper legs. Reference value,  $5.58 \times 10^{-12}$ .

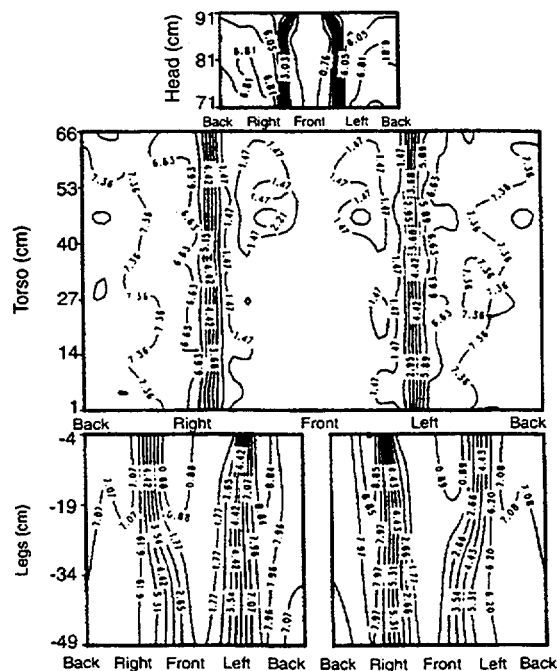


Figure 5. Contour plot for normalised dosimeter response exposed to 0.08 MeV PA beam source for different dosimeter locations on the head, torso, and upper legs. Reference value,  $0.68 \times 10^{-12}$ .

W. D. REECE and X. G. XU

a dosimeter located on the front at the same height is about 10% for 0.08 MeV, 25% for 0.3 MeV, and 40% for 1.0 MeV photon beams. Nevertheless, dosimeters shielded by the body still indicate, to some degree, the radiation to which the body is exposed. These results can help to understand personal monitoring results for situations when the exposure geometry is unknown.

#### Parallel photon beam exposure — PA

Dosimeter readings for PA geometry are presented in Figure 5 for 0.08 MeV photons (results for 0.3 and 1.0 MeV photons are not shown here to save space but can be found in Reference 6). The values of the contour lines on the back are greater than 1 because dosimeter readings are normalised to the dosimeter on the front of the chest, which is shielded by the body in this geometry. Allowing for this difference, PA geometry produces results similar to the AP geometry, i.e. dosimeters on the back have similar responses for radiation incident from the rear half of the body, and, therefore, no specific requirement on dosimeter positioning is necessary. Dosimeters on the front of the torso, shielded by the body, show large variations, as with posterior dosimeters under AP geometry.

#### Parallel photon beam exposure — LAT

Figure 6 shows results for 0.08 MeV photon beams for LAT geometry — exposure to broad parallel beams incident from either side of the body (for Figure 6 the beam is from the right side). Located within the region from 'back' to 'right' then to 'front' in these plots, dosimeters exposed to laterally incident radiation show very uniform responses, ranging from approximately 0.9 to 1.1 for all energies considered. Some dosimeters have readings greater than 1 compared to the reference dosimeter because of backscatter contributions. Backscatter contributions can be large for this geometry, especially for low energy photons.

The LAT exposure geometry is interesting to study because dosimeters worn in front of the body are exposed to radiation from large irradiation angles (90° from AP geometry). Traditionally, an ideal dosimeter was supposed to have an isotropic angular response, and, in this study, the dosimeters have exactly this response. Dosimeters having an isotropic angular response and not shielded by the body will respond theoretically in the same way for LAT geometry as for AP geometry considering only primary photons. However, for reference dosimeters (located at the chest's centre), the ratios of absolute dosimeter readings for LAT geometry to the readings for AP geometry are 0.80, 0.95, and 1.06, for 0.08, 0.3, and 1.0 MeV photon beams, respectively. Investigation of these differences revealed that backscatter contributions to a given dosimeter can play a role in the dosimeter's overall response. Compton scattering causes higher energy pho-

tons to be scattered more into the forward direction while lower energy photons are scattered more uniformly in all directions. For 1 MeV photons, the ratio is greater than 1 because the scatter contribution to the reference dosimeter is greater for lateral exposures, in which the interacting photons are scattered preferentially toward the reference dosimeter, than for AP exposures in which the scattered photons are scattered away from the reference dosimeter. For low energy photons, the scattering is more uniform and for lateral exposure the interacting photons are generally further from the reference dosimeter and absorbed by the body.

Compared to these small differences, however, our earlier results<sup>(3)</sup> showed that  $H_E$  for LAT geometry was about 30% to 50% of that for the AP geometry for the same beam fluence, depending on photon energy. Because many of the critical organs and tissues used to calculate  $H_E$  are situated deep within the body, dose  $H_E$  is significantly influenced by attenuation from intervening body tissues when radiation is incident from either side of the body. The dosimeter results here, however, show that the front dosimeters respond essentially the same as dosimeters under AP geometry. Thus, an isotropic dosimeter calibrated with AP exposures overestimates  $H_E$  for LAT exposures by a factor of 2 to 3 depending on photon energy.

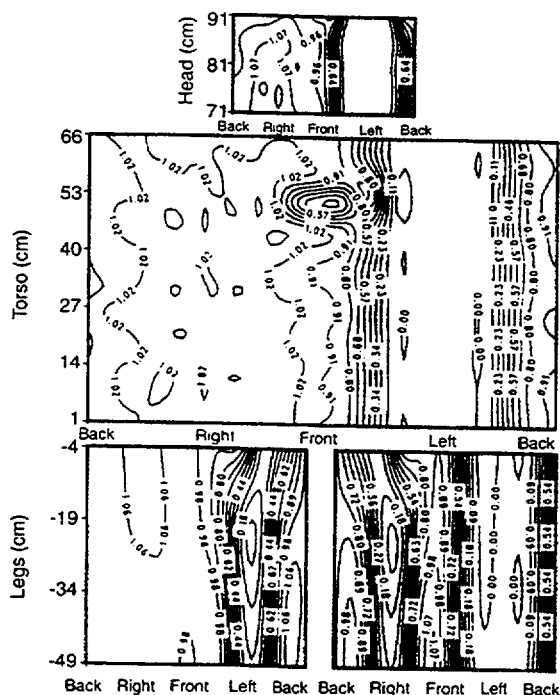


Figure 6. Contour plot for normalised dosimeter response exposed to 0.08 MeV LAT beam source for different dosimeter locations on the head, torso, and upper legs. Reference value,  $0.44 \times 10^{-12}$ .

# $H_E$ FROM PERSONAL DOSEMETERS

## Parallel photon beam exposure — overhead

Figure 7 illustrates results for calculation using 0.08 MeV overhead photon beams. Dosimeter readings are uniform for dosimeters located on the head and torso; the maximum difference is about 20%, 15%, and 8% for 0.08, 0.3, and 1.0 MeV photon beams, respectively. Backscatter from the skull likely causes dosimeters on the head to have slightly higher responses than the ones on the torso. Dosimeters on the legs are partially or completely shielded by the body depending on their distance from the tops of the leg. Depending on the degree of shielding by the body, dosimeters on the legs have relative readings from about 0.5 to almost zero. Earlier results<sup>(3)</sup> indicate that the  $H_E$  from the overhead geometry is about 20% to 33% of that for AP geometry depending on photon energy, due to significant attenuation by outscatter from the upper torso. However, as with LAT geometry, dosimeters exposed by overhead beams show no significant differences in readings from those for the AP geometry. A dosimeter with isotropic angular response placed above the legs would overestimate  $H_E$  from overhead by a factor of 3 to 5 depending on photon energy.

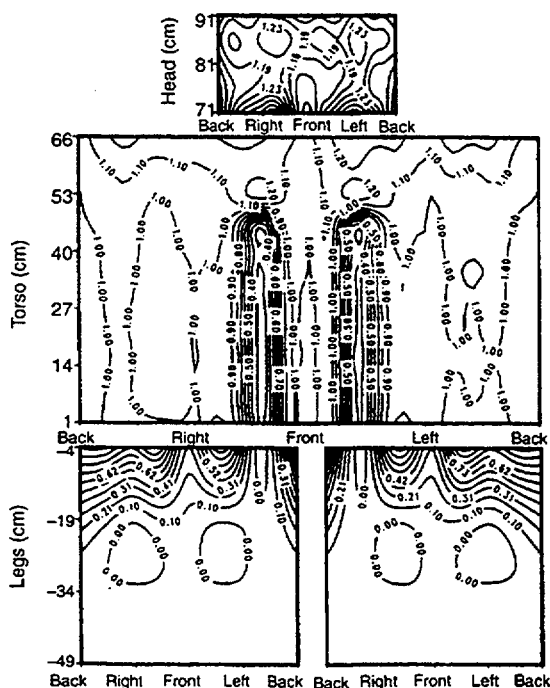


Figure 7. Contour plot for normalised dosimeter response exposed to 0.08 MeV overhead beam source for different dosimeter locations on the head, torso, and upper legs. Reference value,  $0.345 \times 10^{-12}$ .

## Parallel photon beam exposure — underfoot

Results are shown in Figure 8 for exposures from a 0.08 MeV photon beam source below the foot. In this case, dosimeters on the legs and on the torso show fairly uniform readings, ranging from about 0.8 to 1.2 for 0.08 MeV photons and from about 0.9 to 1.1 for 1.0 MeV photons. Dosimeters located on the head are shielded by the torso and show much smaller readings. Considering that  $H_E$  for underfoot exposures is about a third of that for the AP exposure<sup>(3)</sup>, the chest-worn dosimeter with isotropic response overestimates  $H_E$  by a factor of about 3.

## Parallel photon beam exposure — arbitrary

An arbitrary irradiation geometry was modelled by beams incident on the torso having polar angle and azimuthal angles both equal to  $45^\circ$ . This geometry may provide an average response for exposure to parallel photon beams incident from the front half plane of the body. Figure 9 shows the dosimeter reading contour plot for 0.08 MeV photon beams. As with the other exposure geometries discussed before, dosimeters located on the front of the body, and thus directly exposed by the primary photon beam, show responses within about 10% of each other.

Dosimeters that are shielded by the body from this 'double slant' beam show more complicated variations

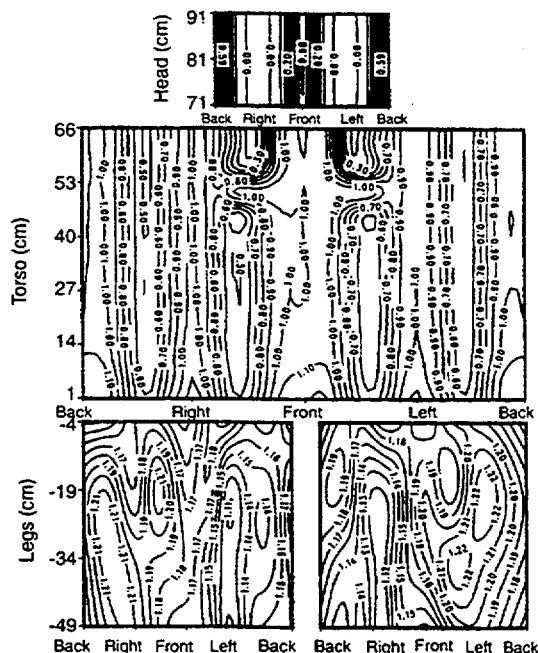


Figure 8. Contour plot for normalised dosimeter response exposed to 0.08 MeV underfoot beam source for different dosimeter locations on the head, torso, and upper legs. Reference value,  $0.335 \times 10^{-12}$ .

in readings than those noted in the perpendicularly incident geometries. However, inspection of these contour plots relative to the incident photon direction suggests that the variations in response by these dosimeters can be explained by considering attenuation and backscatter. The dosimeter reading for a dosimeter at the centre-of-the-back ( $Z = 41$  cm) is 5%, 16%, and 33% of the values of a dosimeter placed at the centre-of-the-chest, for 0.08, 0.3, and 1.0 MeV photon beams, respectively.

### Conclusions on dosimeter positioning

Dosimeter responses for the AP, PA, LAT, overhead, underfoot, and arbitrary exposure geometries provide enough data to draw some general conclusions:

- (1) Location of a dosimeter on the body has little influence on dosimeter reading, provided that the dosimeter is directly exposed to primary radiation.
- (2)  $H_E$  may be underestimated by a dosimeter that is shielded by the body by as much as 90% depending on the photon energy. An additional dosimeter may be needed to avoid underestimate of  $H_E$ .

Strictly, the above conclusions apply only to whole-body exposures to broad parallel photon beams. This source geometry is a common exposure scenario encountered in the workplace. In fact, any source

located reasonably far from the body may be treated as a broad parallel beam geometry. Furthermore, preliminary results from ongoing research indicate that these conclusions, not surprisingly, can also be applied to any large plane source such as a contaminated floor or wall. There are also cases in which dose quantities such as skin dose or extremity dose become more limiting than whole body dose,  $H_E$ . Examples of such exposures are: point sources in contact with the skin or body clothing, and small sources held in the hand. A detailed discussion on these issues is beyond this paper's scope and interested readers are directed to other literature<sup>(17-19)</sup>.

### ALGORITHMS FOR PREDICTING $H_E$ FROM DOSEMETER READINGS

In this section, dosimeter readings are compared with the corresponding  $H_E$  received by a hermaphroditic phantom. Three simple algorithms to relate dosimeter readings to  $H_E$  are developed and the relationships between assessed  $H_E$  from the dosimeter reading and actual  $H_E$  are presented. Table 1 lists ratios of dosimeter response to  $H_E$  received by a hermaphroditic phantom wearing the dosimeters.  $R_F$  is the response of the dosimeter placed on the centre of the chest and  $R_B$  is the response of the dosimeter placed on the centre of the back, both with respect to actual  $H_E$ . The three algorithms to assess  $H_E$  are as follows.

- (1) Algorithm 1 (A1) uses  $R_F$ , the reading from a dosimeter that is placed on the chest, to estimate the  $H_E$ . This algorithm is comparable to the 'one badge' practice that is widely used in the nuclear industry for protection against penetrating radiation. For A1,  $H'_E = R_F$ , where  $H'_E$  is the assessed effective dose equivalent and  $R_F$  is the reading of the dosimeter on the front of the body.
- (2) Algorithm 2 (A2) uses the average of readings from two dosimeters worn on the front of the body and one worn on the back. For A2,  $H'_E = \text{Avg}(R_F, R_B) = (R_F + R_B)/2$ .
- (3) Algorithm 3 (A3) uses two dosimeter readings but weights the highest reading. For A3,  $H'_E = [\text{Max}(R_F, R_B) + \text{Avg}(R_F, R_B)]/2$ , where  $\text{Max}(R_F, R_B)$  stands for the greatest value of  $R_F$  and  $R_B$ .

The ability of these algorithms to predict  $H_E$  from dosimeter readings is summarised in Table 2. Ratios of  $H'_E$  to the actual  $H_E$  received, according to calculations with a hermaphroditic phantom, are given for the selected exposure geometries and photon energies.  $H_E$  is, in fact, the gender-averaged effective dose equivalent. The tabulated data on gender-specific  $H_E$  and the formula for calculating averaged  $H_E$ , were presented earlier<sup>(3)</sup>.

### Algorithm 1

The widespread practice of monitoring with a single dosimeter is perhaps a natural starting point for

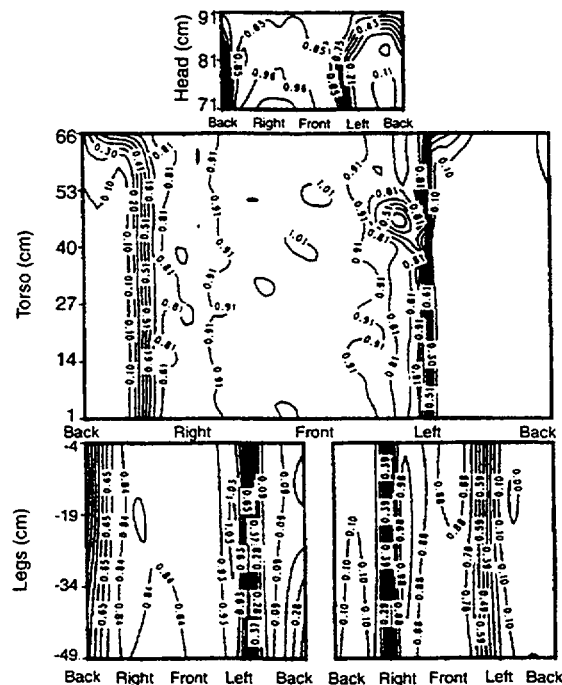


Figure 9. Contour plot for normalised dosimeter response exposed to 0.08 MeV arbitrary beam source ( $A = 45^\circ$  and  $P = 45^\circ$ ), for different dosimeter locations on the head, torso, and upper legs. Reference value,  $0.51 \times 10^{-12}$ .

# $H_E$ FROM PERSONAL DOSEMETERS

algorithm evaluation. The evaluation of this algorithm is discussed for each exposure geometry.

## Parallel photon beam exposure — AP

As seen in Table 2, for AP geometry, perhaps the most common source geometry, the use of A1 will yield a ratio of  $H'_E/H_E$  equal to 1.23, 1.25, and 1.14 for 1.0, 0.3, and 0.08 MeV photons, respectively. In other words, if a worker always faces a photon beam source, then a single dosimeter located on the front of the torso (between the chest and waist) will always slightly overestimate  $H_E$  (within 25%), using the dosimeter reading directly as  $H_E$ . For AP exposure geometry, A1 also gives very consistent results for all energies. Thus  $H_E$  can be assessed with confidence for a wide range of energy spectra.

## Parallel photon beam exposure — PA

For PA exposure, Table 2 shows that A1 underestimates  $H_E$  by about 44%, 61%, and 83% for 1.0, 0.3,

and 0.08 MeV photons, respectively. In general, unfolding the radiation direction by evaluating dosimeter readings is almost impossible, even with dosimeters using sophisticated attenuator arrangements. Thus, A1 is generally not satisfactory when the worker is exposed to the source solely from the back. The chance for a radiation worker to be exposed solely by a posterior source is less than for exposure solely from the front because workers tend to face the radiation source during routine work. For known PA exposure, however, A1 could be corrected by a factor based on the numbers given in Table 2 to estimate  $H_E$  if the photon energy were known.

## Parallel photon beam exposure — LAT

Like the PA geometry, LAT is not as common an exposure geometry as AP geometry. However, LAT geometry is interesting because the beams are incident on both the body and the chest dosimeter at very large angles (about 90° from normal to the dosimeter face). As shown earlier,  $H_E$  for LAT geometry is about 48%,

**Table 1. Ratio of the reading from a dosimeter placed in the front or on the back of the body,  $R_{Front}$  or  $R_{Back}$ , to the actual effective dose equivalent received by a hermaphroditic individual,  $H_E$ , for different irradiation geometries and photon energies.**

Source type	Source geometries	1.0 MeV		0.3 MeV		0.08 MeV	
		$R_{Front}/H_E$	$R_{Back}/H_E$	$R_{Front}/H_E$	$R_{Back}/H_E$	$R_{Front}/H_E$	$R_{Back}/H_E$
Parallel beams	AP	1.23	0.45	1.25	0.32	1.14	0.12
	PA	0.56	1.37	0.39	1.54	0.17	1.34
	LAT	1.76	1.81	2.10	2.11	1.82	1.85
	Overhead <sup>(a)</sup>	2.04	2.02	2.49	2.44	2.25	2.22
	Underfoot	3.35	3.32	3.66	3.59	3.61	3.53
	Arbitrary <sup>(b)</sup>	1.49	0.50	1.71	0.27	1.64	0.08

<sup>(a)</sup>Overhead beam source is achieved by averaging over beams incident from polar angles within polar angle of 15°.

<sup>(b)</sup>Arbitrary geometry is achieved by beams incident from both azimuthal and polar angles equal to 45°.

**Table 2.  $H'_E/H_E$ , ratio of the assessed effective dose equivalent<sup>(a)</sup>,  $H'_E$ , to the actual effective dose equivalent received by a hermaphroditic individual,  $H_E$ , for different exposure geometries and photon energies.**

Source type	Source geometry	1.0 MeV			0.3 MeV			0.08 MeV		
		A1	A2	A3	A1	A2	A3	A1	A2	A3
Parallel beams	AP	1.23	0.87	1.05	1.25	0.79	1.02	1.14	0.63	0.89
	PA	0.56	0.97	1.17	0.39	0.96	1.25	0.17	0.76	1.05
	LAT	1.76	1.79	1.80	2.10	2.11	2.11	1.82	1.83	1.84
	Overhead <sup>(b)</sup>	2.04	2.03	2.04	2.49	2.47	2.48	2.25	2.24	2.24
	Underfoot	3.35	3.33	3.34	3.66	3.64	3.65	3.61	3.57	3.60
	Arbitrary <sup>(c)</sup>	1.49	0.99	1.24	1.71	0.99	1.35	1.64	0.86	1.25

<sup>(a)</sup>For A1,  $H'_E = R_{Front}$ . For A2,  $H'_E = \text{Avg. } (R_{Front}, R_{Back})$ . For A3,  $H'_E = [\text{Max. } (R_{Front}, R_{Back}) + \text{Avg. } (R_{Front}, R_{Back})]/2$ .

<sup>(b)</sup>Overhead beam source is achieved by averaging over beams incident from polar angles within polar angle of 15°.

<sup>(c)</sup>Arbitrary geometry is achieved by beams incident from both azimuthal and polar angles equal to 45°.

W. D. REECE and X. G. XU

57%, and 71% of that for AP geometry for 0.08, 0.3, and 1.0 MeV photons, respectively. Dosimeters with isotropic responses will obviously overestimate  $H_E$  by up to a factor of 2 in LAT geometry. Table 2 indicates that A1, indeed, gives a  $H'_E/H_E$  ratio of 1.76, 2.1, and 1.82 for 1.0, 0.3, and 0.08 MeV photons, respectively. The response of a commercial dosimeter, however, is not strictly isotropic and may be smaller at large angles. For LAT geometry, A1 consistently overestimates  $H_E$  by almost a factor of 2, assuming isotropic angular responses. More accurate assessments of  $H_E$  could be achieved by requiring proper angular response functions in dosimeter design and calibration<sup>(20)</sup>.

#### Parallel photon beam exposure — overhead

An example of overhead geometry could be a worker in a steam generator channel head plugging tubes in the tube sheet during an outage. For this exposure geometry, the US worker is required to wear dosimeters on the head and elsewhere on the torso in order to report the highest dose as the dose of record<sup>(7-9)</sup>. Table 2 shows that A1 (using a single dosimeter at chest area) already consistently overestimates the  $H_E$  for this exposure geometry; the ratio,  $H'_E/H_E$ , is 2.04, 2.49, and 2.25 for 1.0, 0.3, and 0.08 MeV photons, respectively. The overhead source geometry presented in Table 2 is the average of beams incident from polar angles between 0° and 15° to allow for slightly different orientations of the body under this exposure geometry. Again, an isotropic angular response of the dosimeter was used in the calculations. Clearly, the requirement by USNRC to report the highest dose anywhere on the torso is overly conservative and produces to a poor estimate of risk from this exposure geometry.

#### Parallel photon beam exposure — underfoot

Underfoot beam exposures could arise when workers are exposed to a contamination source on the floor sufficiently below the body. The photons from a point source on the floor are sufficiently parallel by the time they reach the torso that underfoot beam conditions apply with little error. Table 2 indicates that the  $H'_E/H_E$  ratio is 3.35, 3.66, and 3.61 for 1.0, 0.3, and 0.08 MeV photons, respectively, when A1 is used. These consistent overestimates are as expected for dosimeters with isotropic response, because  $H_E$  for underfoot beam sources is about 30% of that for AP geometry but the dosimeter response does not change significantly between AP and underfoot geometries.

#### Parallel photon beam exposure — arbitrary

For 'arbitrary' irradiation geometry with beams incident on the torso with polar and azimuthal angles both set to 45°, the  $H'_E/H_E$  ratio is higher than those for AP geometry for the same photon energy. This means that,

for beams incident from the front but not the AP geometry, the  $H'_E$  is overestimated even more than for AP geometry. This phenomena arises because  $H_E$  decreases rapidly as the beam departs from AP geometry within the front half plane, but isotropic dosimeter readings change little with beam angle. A1 always overpredicts  $H_E$  for all frontally incident photon beams.

In summary, for all exposures considered, A1 is consistently conservative in assessing  $H_E$ , except for PA for which the front-worn dosimeter is shielded by the body. It may not be possible to avoid a dosimeter being shielded by the body (or to correct readings from such a dosimeter), especially when the radiation sources are not identifiable, or a worker is changing orientation in the radiation field, or other factors. Fortunately, in the workplace, the overestimates of  $H_E$  for other exposure geometries are generally greater than the underestimate for PA geometry, and the overall assessed  $H_E$  (e.g. the average of all exposures) is usually still conservative. The data suggest that the practice of using a single badge for personal monitoring is generally satisfactory for routine exposures.

To avoid underestimation from a dosimeter being shielded by the body, two dosimeters could be used, one on the front of the body and another one on the back. This two-dosimeter approach ensures that there is at least one dosimeter which is not shielded by the body at all times. Algorithms 2 and 3, based on two dosimeters, are discussed next.

#### Algorithm 2

Algorithm 2 (A2) assumes two isotropic dosimeters, one worn on the front of the body and one on the back. For A2, the assessed effective dose equivalent is given by the average of readings from these two dosimeters, i.e.  $H'_E = (R_F + R_B)/2$ . As shown in Table 2, A2 completely avoids the underestimate of  $H_E$  by A1 when used for PA beam geometry. A2 also improves the precision of the results for certain geometries (e.g. for the arbitrary geometry). However, A2 underestimates for the AP beam geometry for all photon energies. Nevertheless, the underestimation is still well within the allowed range of accuracy (a factor of 1.5) recommended by the ICRP<sup>(21)</sup>. This algorithm does not significantly change the results for LAT, overhead, and underfoot geometries for which the two dosimeters with isotropic angular responses show similar readings.

#### Algorithm 3

Algorithm 3 (A3) uses the same two dosimeter readings as A2, but weights the higher reading dosimeter more. The assessed effective dose equivalent is given by:  $H'_E = [\text{Max}(R_F, R_B) + \text{Avg}(R_F, R_B)]/2$ , where  $\text{Max}(R_F, R_B)$  stands for the higher value of  $R_F$  and  $R_B$ . This expression reduces to  $H'_E = [0.75 \text{Max}(R_F, R_B) + 0.25 \text{Min}(R_F, R_B)]$ . Obviously, A3 produces more conserva-

#### $H_E$ FROM PERSONAL DOSEMETERS

tive results overall than those obtained using A2; the ratio,  $H_E/H_E$  is, at worst, only slightly smaller than unity (i.e. underpredicts  $H_E$ ) for all exposure geometries and photon energies.

#### Recommendations on the use of algorithms

In routine operations, most workers are likely to face the radiation source and A1 produces satisfactory assessment of  $H_E$ . The current single-badge approach is, therefore, acceptable for routine use. For A1, the dosimeter can be worn either in the chest area or at the waist level.

For special circumstances involving multidirectional exposures, nuclear power plants are already providing special dosimeters, and the evaluation of the A2 and A3 shows that, for whole-body exposure (as opposed to part-body exposure), only two dosimeters are needed, with a proper algorithm, to assess  $H_E$  satisfactorily. No placement requirements are necessary, except that one dosimeter should be placed on the front of the body and another is placed on the back of the body. The use of A2 and A3 does not require significant modification to current dosimetry practices. If these algorithms are accepted by the USNRC, nuclear plants may be able to save money and manpower, yet provide satisfactory assessment of  $H_E$  for their work force.

Very accurate assessments of  $H_E$  can be achieved using the tabulated photon-fluence-to- $H_E$  conversion factors published earlier directly for known beam and point sources<sup>(3)</sup>. For interpreting dosimeter readings, one should remember that the dosimeter readings calculated in this study are only an indication of the readings from a commercially available dosimeter which was assumed to be made from or calibrated to tissue-equivalent material. Also, the angular dependence and attenuation by the dosimeter capsule were not considered. Thus, the values given in the Table 2 may not be directly applicable for converting dosimeter readings into  $H_E$ . In practice, calibrations are required to take into account the configuration, material, and angular depen-

dence of commercial dosimeters which are beyond the scope of this study. Dosimeters can be designed to have proper angular responses following the angular dependence characteristics of  $H_E$  at off-normal incident angles, thereby yielding more accurate personal monitoring results. Reference on this issue can be found elsewhere<sup>(20)</sup>. The results from this study are easily extended to use the weighting factors described in ICRP 60<sup>(22)</sup>. For most irradiation geometries, the calculated doses are smaller using the ICRP 60 weighting factors compared to the ICRP 26 values for the same exposure. In general, the methods described in this paper will be conservative for the ICRP 60 factors.

#### CONCLUSIONS

Effective dose equivalent ( $H_E$ ), defined in ICRP Publication 26 and adopted by the USNRC, was calculated for 0.08, 0.3, and 1.0 MeV external photon sources using the MCNP computer code and anthropomorphic phantoms. A large number of exposure geometries were investigated which expands the existing data and thus allows a better estimate of radiation risk to radiation workers exposed to external photon radiation.

Dosimeter response simulations indicate that location of a dosimeter has small influence on dosimeter responses, provided that the dosimeter is directly exposed to primary radiation. A dosimeter which is shielded by the body may under-respond by 60% to 90% for photon energies from 1.0 MeV to 0.08 MeV at AP geometry. However, by wearing two dosimeters, one on the front and one on the back, underestimation of  $H_E$  can be avoided in many special exposure situations. For situations when doses become higher or less predictable, gradually more complex or realistic monitoring procedures should be adopted. These include detailed characterisation of the direction, energy, and type of the radiation, the habits of a worker in body orientation in the radiation field, and the placement of dosimeters. The photon-fluence-to- $H_E$  conversion factors provided in Reference 3, along with personal dosimeter readings, can be applied to construct organ doses and  $H_E$  quite accurately.

#### REFERENCES

1. US Nuclear Regulatory Commission (USNRC). *Title 10 Part 20 of the Code of Federal Regulations (10 CFR 20), Standard for Protection Against Radiation* (Washington, DC: USNRC) (21 August 1991).
2. International Commission on Radiological Protection. *Recommendations of the International Commission on Radiological Protection* (Oxford, England: Pergamon Press) ICRP Publication 26 (1977).
3. Reece, W. D., Poston, J. W. and Xu, X. G. *Determining the Effective Dose Equivalent for External Photon Radiation. Calculational Results for Beam and Point Source Geometries*. Radiat. Prot. Dosim. 55(1), 5-21 (1994).
4. Radiation Shielding Information Center (RSIC). *MCNP 4: Monte Carlo Neutron and Photon Transport Code System* (Oak Ridge, TN: Oak Ridge National Laboratory) Report CCC-200A (1991).
5. Cristy, M. and Eckerman, K. F. *Specific Absorbed Fractions of Energy at Various Ages from Internal Photon Sources* (Oak Ridge, TN: Oak Ridge National Laboratory) ORNL/TM-8381/V1 (1987).
6. Xu, X. G. *The Assessment of Effective Dose Equivalent using Personnel Dosimeters*. Ph.D. Dissertation, Nuclear Engineering/Health Physics, Texas A&M University (May 1994).
7. US Nuclear Regulatory Commission (USNRC). *Placement of Personnel Monitoring Devices for External Radiation* (Washington, DC: USNRC) IEN 81-26 (1981).

W. D. REECE and X. G. XU

8. US Nuclear Regulatory Commission (USNRC). *Dose Assignment for Workers in Non-uniform Radiation Fields* (Washington, DC: USNRC) IEN 83-95 (1983).
9. Hudson, C. G. *The Need for Dosimetry Multibadging at Nuclear Power Plants*. Radiat. Prot. Manage. January, 43-49 (1984).
10. Jones, K. L., Roberson, P. L., Fox, R. A., Cummings, F. M. and McDonald, J. C. *Performance Criteria for Dosimeter Angular Response* (Richland, WA: Pacific Northwest Laboratories) PNL-6452 (1988).
11. National Council on Radiation Protection and Measurements. *Use of Personal Monitors to Estimate Effective Dose Equivalent and Effective Dose Equivalent and Effective Dose to Workers for External Exposure to Low-LET Radiation*. NCRP Report No. 122, National Council on Radiation Protection and Measurements, Bethesda, Maryland.
12. Hertel, N. E. and McDonald, J. C. *Methods for the Calibration of Photon Personnel Dosimeters in Terms of the Ambient Dose Equivalent*. Radiat. Prot. Dosim. 32(3), 149-156 (1990).
13. Austerlitz, C. Kahn, B., Eichholz, G. G., Zankl, M. and Drexler, G. *Calculation of the Effective Male Dose Equivalent Relative to the Personal Dose at Nine Locations with a Free-arm Model*. Radiat. Prot. Dosim. 36(1), 13-21 (1991).
14. Attix, F. H. *Introduction to Radiological Physics and Radiation Dosimetry* (New York: John Wiley) (1986).
15. Hubbell, J. H. *Photon Mass Attenuation and Mass Energy-Absorption Coefficients from 1 keV to 20 MeV*. Int. J. Appl. Radiat. Isot. 33, 1269-1290 (1982).
16. International Commission on Radiation Units and Measurements. *Radiation Quantities and Units* (Bethesda, MD: ICRU Publications) Report 33 (1980).
17. International Commission on Radiation Units and Measurements. *Measurement of Dose Equivalents from External Photon and Electron Radiation* (Bethesda, MD: ICRU) ICRU Report 47 (1992).
18. Reece, W. D., Backenbush, L. W. and Roberson, P. L. *Extremity Monitoring: Considerations in Use, Dosimeter Placement, and Evaluation* (Germantown, MD: Nuclear Regulatory Commission) NUREG/CR-9279 (1985).
19. National Council on Radiation Protection and Measurements. *Limit for Exposure to "Hot Particles" on the Skin* (Bethesda, MD: NCRP) NCRP Report No 106 (1989).
20. Xu, X. G., Reece, W. D. and Poston, J. W. *The Study of Angular Dependent Problem in Effective Dose Equivalent Assessment Using Anthropomorphic Phantoms*. Health Phys. 68, 214-224 (1995).
21. International Commission on Radiological Protection. *General Principles of Monitoring for Radiation Protection of Workers*. (Oxford: Pergamon Press) ICRU Report 35 (1982).
22. International Commission on Radiological Protection. *1990 Recommendations of the International Commission on Radiological Protection*, ICRP Publication 60, Annals of the ICRP, 21, Pergamon Press, Elmsford, New York.

*Target:*


Nuclear Power Full Group Purchase

**About EPRI**

EPRI creates science and technology solutions for the global energy and energy services industry. U.S. electric utilities established the Electric Power Research Institute in 1973 as a nonprofit research consortium for the benefit of utility members, their customers, and society. Now known simply as EPRI, the company provides a wide range of innovative products and services to more than 700 energy-related organizations in 40 countries. EPRI's multidisciplinary team of scientists and engineers draws on a worldwide network of technical and business expertise to help solve today's toughest energy and environmental problems.

EPRI. Powering Progress

© 1998 Electric Power Research Institute (EPRI), Inc. All rights reserved. Electric Power Research Institute and EPRI are registered service marks of the Electric Power Research Institute, Inc. EPRI. POWERING PROGRESS is a service mark of the Electric Power Research Institute, Inc.

 Printed on recycled paper in the United States of America

TR-109446